ORGANOMETALLICS

Article

pubs.acs.org/Organometallics

Conformational Properties of 1-Halogenated-1-Silacyclohexanes, $C_5H_{10}SiHX$ (X = Cl, Br, I): Gas Electron Diffraction, Low-Temperature NMR, Temperature-Dependent Raman Spectroscopy, and Quantum-Chemical Calculations†

Sunna Ó. Wallevik,[‡,⊥] Ragnar Bjornsson,[‡,#] Ágúst Kvaran,[‡] Sigridur Jonsdottir,[‡] Ingvar Arnason,*[,‡] Alexander V. Belyakov,[§] Thomas Kern,[∥,▽] and Karl Hassler[∥]

[‡]Science Institute, University of Iceland, Dunhaga 3, IS-107 Reykjavik, Iceland

[§]Saint-Petersburg State Technological Institute, Saint-Petersburg 190030, Russia

[∥]Technische Universität Graz, Stremayergasse 16, A-8010 Graz, Austria

Supporting Information

ABSTRACT: The molecular structures of axial and equatorial conformers of *cyclo*-$C_5H_{10}SiHX$ (X = Cl, Br, I) as well as the thermodynamic equilibrium between these species was investigated by means of gas electron diffraction, dynamic nuclear magnetic resonance, temperature-dependent Raman spectroscopy, and quantum-chemical calculations applying CCSD(T), MP2, and DFT methods. According to the experimental and calculated results, all three compounds exist as a mixture of two chair conformers of the six-membered ring. The two chair forms of C_s symmetry differ in the axial or equatorial position of the X atom. In all cases, the axial conformer is preferred over the equatorial one. When the experimental uncertainties are taken into account, all of the experimental and theoretical results for the conformational energy ($E_{axial} - E_{equatorial}$) fit into a remarkably narrow range of −0.50 ± 0.15 kcal mol^{-1}. It was found by NBO analysis that the axial conformers are unfavorable in terms of steric energy and conjugation effects and that they are stabilized mainly by electrostatic interactions. The conformational energies for $C_6H_{11}X$ and *cyclo*-$C_5H_{10}SiHX$ (X = F, Cl, Br, I, At) were compared using CCSD(T) calculations. In both series, fluorine is predicted to have a lower conformational preference (cyclohexane equatorial, silacyclohexane axial) than Cl, Br, and I. It is predicted that astatine would behave very similarly to Cl, Br, and I within each series.

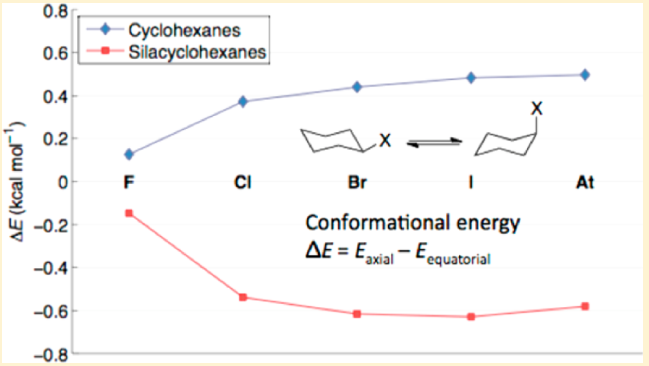

INTRODUCTION

The stereochemistry of cyclohexane (**1**) is among the best-explored areas in organic stereochemistry.[2,3] The chair-to-chair inversion in cyclohexane is well-understood, and the Gibbs free energy of activation for the step chair → half-chair‡ → twist is generally accepted to be 10.1−10.5 kcal mol^{-1}. Far fewer investigations have been reported on silicon-containing six-membered rings. In silacyclohexane (**6**), the activation energy is about one-half of the value for cyclohexane.[4,5] The conformational equilibria of a large number of monosubstituted cyclohexanes have been studied. Winstein and Holness defined the *A* value as the thermodynamic preference for the equatorial conformation over the axial one (see Scheme 1 for the definition of *A*).[6] A positive *A* value corresponds to a preference for the equatorial conformer, and $\Delta G = G_{ax} - G_{eq} > 0$. All energy differences herein will be presented as (axial − equatorial). As a rule, in monosubstituted cyclohexanes, the substituent prefers the equatorial position of the chair conformation. Rare exceptions are substituents having mercury bonded to the cyclohexane ring. When the substituent becomes bulkier its equatorial preference generally increases. The simplest alkyl groups (methyl, ethyl, isopropyl, and *tert*-butyl)

Scheme 1

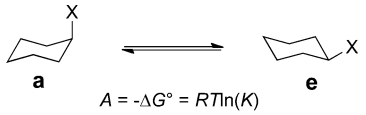

1: R = H
2: R = F
3: R = Cl
4: R = Br
5: R = I

6: R = H
7: R = F
8: R = Cl
9: R = Br
10: R = I

Received: June 18, 2013
Published: November 15, 2013

   dx.doi.org/10.1021/om4005725 | *Organometallics* 2013, 32, 6996−7005

have been used as examples. This tendency has in a classical way been ascribed to 1,3-syn-axial interactions between the substituent in the axial position and axial hydrogens on the ring carbon atoms at positions 3 and 5.[7] Toward the end of the last century, the accepted *A* values were 1.74, 1.79, 2.21, and 4.9 kcal mol^{-1} for Me, Et, *i*-Pr, and *t*-Bu, respectively.[8−10] Evidence questioning the model of 1,3-syn-axial interactions is starting to appear. Wiberg et al.[11] revised the *A* values for the three lightest alkyl groups and reported values of 1.80, 1.75, and 1.96 kcal mol^{-1} for Me, Et, and *i*-Pr, respectively (all values reported with the error limit of ±0.02 kcal mol^{-1}), and the authors concluded that there was no evidence of 1,3-syn-axial interactions with the axial hyrogens of C3 and C5. Taddei and Kleinpeter examined the role of hyperconjugation in substituted cyclohexanes.[12,13] Using atoms in molecules (AIM) analysis, Cuevas and co-workers concluded that the *t*-Bu group is more stable when it adopts the axial position in cyclohexane but produces destabilization of the cyclohexyl ring.[14] Clearly the conformational preferences in monosubstituted cyclohexanes are not fully understood. In recent years, *A* values for some monosubstituted derivatives of **6** have been reported. Methyl[15−18] and phenyl[19] substituents were found to have positive *A* values, albeit much lower in magnitude than for the corresponding cyclohexane analogues.[20−22] Other substituents such as CF_3[23,24] and SiH_3[25] were found to prefer the axial position, contrary to their cyclohexane analogues.

Theoretical studies have confirmed the increased preference for the axial position when monosubstituted silacyclohexanes are compared with monosubstituted cyclohexanes.[26,27] A unified model that can explain the conformational properties of both ring systems has not yet been presented. Therefore, more information would be valuable. The *A* values of the halocyclohexanes **2**−**5** have been reported a number of times using different methods (for a summary of the data, see refs 9 and 20). The experimental and theoretical *A* values for **2** vary from 0.1 to 0.4 kcal mol^{-1} depending on the method, but most of the experimental values lie between 0.2 and 0.3 kcal mol^{-1}. Most of the values for **3**, **4**, and **5** are close to 0.5 kcal mol^{-1}. The fluoro compound **7** has been studied extensively by our group, applying not only experimental methods such as gas electron diffraction (GED), dynamic nuclear magnetic resonance (DNMR), microwave spectroscopy (MW), and temperature-dependent Raman spectroscopy but also quantum-chemical (QC) calculations.[28,29] A separate infrared and Raman study has recently appeared.[30] An axial preference for the F substituent (*A* values from −0.1 to −0.5 kcal mol^{-1}) was manifested by all of the experimental methods and calculations. We then embarked upon a comprehensive study of the conformational properties of the chloro-, bromo-, and iodo-substituted silacyclohexanes (**8**−**10**, respectively). In this paper, we present results from GED, DNMR, and Raman experiments as well as QC calculations. The GED experiment for compound **10**[31] has been reported separately, and short notices of the GED results for **8**[32] and **9**[33] have been given. Recently, a separate study by Klaeboe and co-workers on the vibrational spectra (infrared and Raman) of 1-chlorosilacyclohexane (**8**) has been published.[34]

RESULTS AND DISCUSSION

GED Analysis. Structure refinements of compounds **8** and **9** were carried out with least-squares analyses of the experimental molecular intensity curve *sM*(*s*). According to QC calculations, two stable conformers of $C_5H_{10}SiHX$ exist: axial (ax) and equatorial (eq). Each form possesses C_s symmetry with a chair conformation of the six-membered ring. The radial distribution functions for **8** and **9** are shown in Figures 1 and 2, respectively.

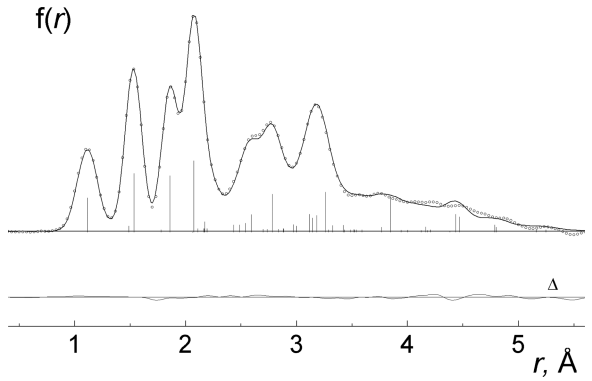

Figure 1. (top) Experimental (open circles) and calculated (solid lines) radial distribution curves of the $C_5H_{10}SiHCl$ molecule. (bottom) Difference curve for the optimized mixture of the conformers.

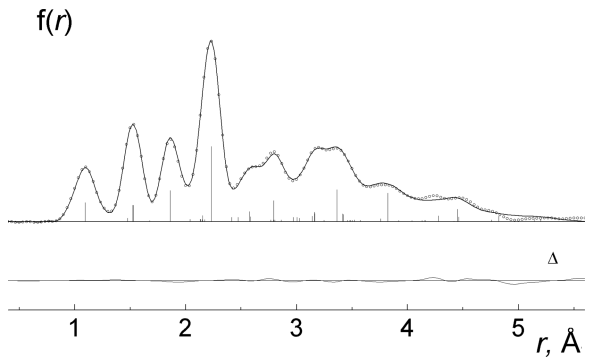

Figure 2. (top) Experimental (open circles) and calculated (solid lines) radial distribution curves of $C_5H_{10}SiH-Br$ molecule. (bottom) Difference curve for the optimized mixture of the conformers.

Important structural parameters along with the equilibrium compositions in the gas phase are given in Table 1 for **8**, **9**, and **10**. In all cases there is a clear preference for the axial form. A structural model of the axial form along with atomic numbering is shown in Figure 3.

As can be seen from Table 1 and ref 28, the Si−C bond is enlarged in the series $C_5H_{10}SiHX$ with X = F, Cl, Br, and I, starting from 1.854(2) Å for X = F through 1.859(2), 1.860(2) to 1.868(5) Å, respectively. This may be rationalized with the use of Bent's rule,[35] according to which a central atom tends to direct hybrids of higher p character toward the more electronegative substituents. This leads to higher s character of the hybrids directed toward the less electronegative substituents attached to the same central atom. Because the size of hybrids of higher p character is larger than those of higher s character, the bonds adjacent to the more electronegative substituent have to become shorter. Hence, the Si−C bond has to become shorter as the electronegativity of the halogen atom increases in going from I to F.

NMR Spectroscopy. Above about 140 K, the ^{13}C NMR spectra show rapid inversion of all of the compounds **8**−**10**. Upon cooling below 140 K, the spectra show significant line broadening and gradual splitting of the signals into two components, indicating a mixture of two conformers. This effect is shown in Figure 4 for carbons C3 and C5 in compound

dx.doi.org/10.1021/om4005725 | *Organometallics* 2013, 32, 6996−7005

Table 1. Structural Parameters of 1-Halo-1-silacyclohexane Molecules by Gas-Phase Electron Diffraction[a]

	X = Cl (**8**)	X = Br (**9**)	X = I (**10**)
$-\Delta G^{\circ}_{298}$ (kcal mol^{-1})[b]	−0.43(18)	−0.82(21)	−0.59(22)
χ_{ax} (%)[b]	67(5)	80(5)	73(7)
	Bond Lengths (Å)		
Si−C	1.859(2)	1.860(2)	1.868(5)
Si−X_{ax}	2.073(2)	2.232(2)	2.458(6)
Si−X_{eq}	2.063(2)	2.221(2)	2.447(6)
C2−C3	1.534(3)	1.528(3)	1.535(9)
C3−C4	1.529(3)	1.523(3)	1.528(9)
$(C-H)_{av}$	1.116(4)	1.103(3)	1.090(8)
	Bond Angles (deg)[c]		
C2−Si−C6	107.7(6)	106.2(4)	105.5(10)
C3−C4−C5	116.8(15)	116.7(7)	112.2(26)
$(H-C-H)_{av}$	106.4[d]	106.8[d]	106.8[d]
C2−C3−C4	114.2(7)	115.5(9)	114.1(13)
Si−C2−C3	110.3(4)	111.0(3)	110.2(7)
X−Si−C2	110.3(5)	109.7(3)	109.3(10)
C2−Si−C6−C5	−42.2(15)	−42.6(8)	−42.6(27)
Si−C6−C5−C4	51.6(12)	51.3(7)	55.8(18)
C6−C5−C4−C3	−62.7(14)	−59.6(16)	−67.4(26)

[a]Atom numbering is shown in Figure 3. The *R* factors are 5.9, 5.4 and 9.5% for **8**, **9**, and **10**, respectively. Values in parentheses are 3σ. [b]Relative standard free energy ($-\Delta G^{\circ}$) and mole fraction (χ). [c]H_{ax}−C2−C3 = H_{eq}−C3−C2 = H_{eq}−C3−C4 = H_{ax}−C3−C2. [d]Fixed.

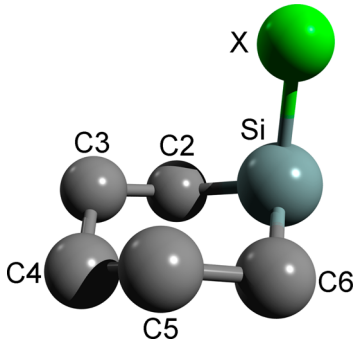

Figure 3. Molecular model and atom numbering.

8. The low-temperature spectra of **9** and **10** follow the same pattern. The higher-field (lower δ) component signal is much larger in all cases. In previous work on related compounds, we have shown that the ^{13}C chemical shifts of the ring carbon atoms C3 and C5 have lower δ values when the substituent is in the axial position compared with that in the equatorial one.[15,25] The same results have been derived by computational studies for **8**, **9** and **10**. On the basis of the ^{13}C NMR signal weights (hence relative populations) and QC chemical shift calculations, we conclude that the same holds for the C2(6) and C3(5) ring carbon atoms. No clear splitting of the C4 signals is observed, whereas the QC chemical shift calculations predict the ring C4 atoms to have slightly higher δ values when the substituent is in the axial position compared with the equatorial one. For more information, see the Experimental Section and the Supporting Information.

Dynamic NMR simulations of the spectra obtained using the software WinDNMR,[36] as shown in Figure 4, allowed the determination of the rate constants ($k_{e\rightarrow a}$) and the corresponding free energies of activation ($\Delta G^{\ddagger}_{e\rightarrow a}$) as functions of temperature. The most reliable results were obtained from

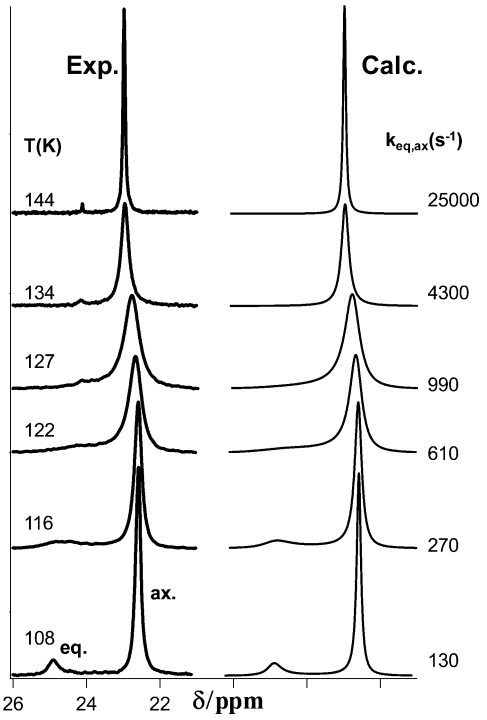

Figure 4. Simulation of the ^{13}C NMR signals for C3 and C5 of compound **8** in a mixture of CD_2Cl_2, $CHFCl_2$, and CHF_2Cl in a ratio of 1:1:3 at low temperatures. Experimental spectra are on the left, and calculated spectra are on the right.

the C3(5) pair of carbon atoms. Chemical shifts derived from the NMR spectra recorded at the lowest temperatures were assumed to represent conditions of negligible ring inversion. Average values for $\Delta G^{\ddagger}_{e\rightarrow a}$ are listed in Table 2. The equilibrium

Table 2. Parameters Relevant to Conformational Equilibria and Rates of Exchange Derived from Dynamic NMR Simulations of ^{13}C NMR spectra (C3 and C5 Atoms)

parameter	**8**	**9**	**10**
coalescence point (K)	127(5)	132(5)	132(5)
$\Delta G^{\ddagger}_{e\rightarrow a}$ (kcal mol^{-1})[a]	5.3(1)	5.4(2)	5.4(2)
$K_{e\rightarrow a}$[b]	4.88(4)	5.99(4)	5.99(4)
$\Delta G_{e\rightarrow a}$ (kcal mol^{-1})[c]	−0.35(3)	−0.40(3)	−0.40(3)

[a]Average values over the temperature ranges 107−150 K (**8**), 110−150 K (**9**), and 113−132 K (**10**). [b]$K_{e\rightarrow a}$ is the equilibrium constant for the equatorial to axial inversion derived from ax:eq signal intensity ratios over the temperature ranges specified in footnote *a*. [c]$\Delta G_{e\rightarrow a} = -RT\ln(K_{e\rightarrow a})$ at T = 128.5 K.

constants ($K_{e\rightarrow a}$), and hence the free energy changes ($\Delta G_{e\rightarrow a}$), for the equatorial to axial transformations at temperatures close to the coalescence points were determined from the relative signal intensities (Table 2).

Raman Spectroscopy. In previous publications, we used temperature-dependent Raman spectroscopy to analyze the ratio of axial and equatorial conformers in Si-substituted silacyclohexanes.[17,25,28,37] The application of the method to this problem has been described in detail in one of the publications,[25] and therefore, only a brief description will be given here. Temperature-dependent Raman spectra of compounds are typically analyzed using the van't Hoff relation, $\ln(A_1/A_2) = -\Delta H/RT$ + constant, where A_1 and A_2 are the intensities of the vibrational bands belonging to two different

dx.doi.org/10.1021/om4005725 | *Organometallics* 2013, 32, 6996−7005

conformers of the molecule. Either the heights or areas of the bands can be used for the A_1/A_2 ratio. The relation is correct under the assumption that ΔH and the Raman scattering coefficients are temperature-independent.

In our previous reports on related silacyclohexanes, we used pairs of Raman bands belonging to the axial and equatorial conformers. As a rule, the symmetric Si−C2(6) stretching mode and/or the Si−X stretching mode (X = substituent) have been found to be well or moderately well separated in the sample spectrum, and the intensity ratio has shown variation with temperature. Assignment to the axial or equatorial conformer is made by comparison with calculated vibrations.

In this contribution, we used the Si−X (X = Cl, Br, I) stretching vibrations for the axial and equatorial conformers for all of the compounds **8**−**10**. The experimental and calculated frequencies are summarized in Table 3.

Table 3. Experimental (Room Temperature) and Calculated Si−X Stretching Frequencies for Compounds 8, 9, and 10 (cm^{-1})

	experimental		calculated[a]	
	axial	equatorial	axial	equatorial
8	474	538	472	537
9	389	432	391	436
10	324	402	313	394

[a]B3LYP[38,39]/6-31+G(d,p)[40−45] for **8** and **9**, B3LYP/aug-cc-pVDZ[46,47] for **10**.

Low-temperature spectra were recorded for pure **8** and **9** at temperatures varying from 300 to 195 K at 15 K intervals. Spectra were also recorded for the two compounds in THF and heptane solution. Low-temperature spectra were recorded for pure **10** and for **10** in toluene solution at temperatures varying from 290 to 190 K at 10 K intervals.

Signal overlap makes the Raman spectra of **8** and **10** somewhat more complicated in the Si−X stretching region than the spectrum of **9**. Shown in the bottom panel of Figure 5 is the room-temperature Raman spectrum of neat **10** over the wavenumber range 200−800 cm^{-1}; the middle panel shows the expanded spectrum over the range 300−420 cm^{-1}, and calculated spectra over the 280−420 cm^{-1} range are shown in the upper panel. More information on band deconvolution and the temperature dependence of the spectra of the three compounds is given in the Supporting Information. Figure 6 shows the van't Hoff plots for the 324/402 cm^{-1} band pair of pure **10** using both peak heights (top panel) and peak areas (bottom panel).

The resulting ΔH values are listed for compounds **8**−**10** in Tables 4, 5, and 6, respectively. The listed entries are averaged values from measured peak heights and peak areas. We estimate that ±0.15 kcal mol^{-1} is a fair limit for the error involved in the ΔH results. We note that the polarity of the solvent does not significantly influence ΔH. We also note that our results for **8** are in good agreement with the average value reported by Klaeboe and co-workers (−0.67 kcal mol^{-1}) using other band pairs.[34]

COMPUTATIONAL STUDIES

The minimum-energy pathways for the chair-to-chair inversion of compounds **8**, **9**, and **10** (and **7** for comparison) are shown in Figure 7 and are overall very similar. Similarly to previous

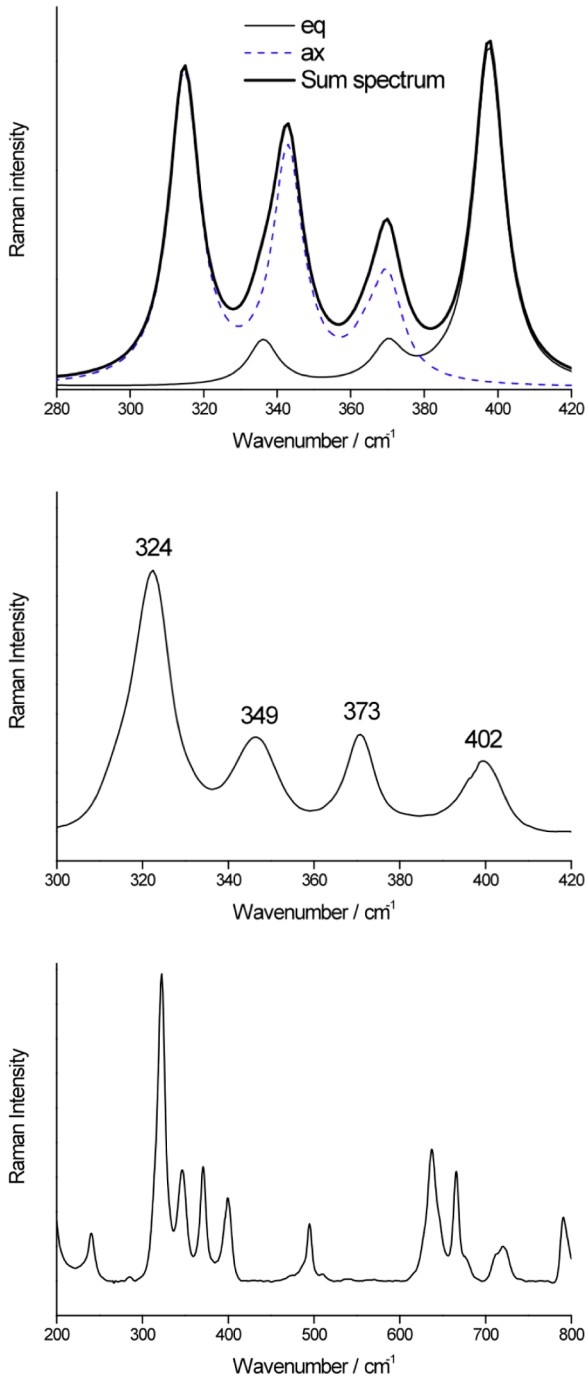

Figure 5. Raman spectrum of $C_5H_{10}SiHI$ over the range 200−800 cm^{-1} (bottom), expanded spectrum over the range 300−420 cm^{-1} (middle), and calculated spectra over the range 280−420 cm^{-1} (top).

silacyclohexanes, the inversion path starting from the axial conformer consists of a half-chair/sofa-like transition state from which the molecule can move into a twist form of relatively high energy. The molecule then goes through a boat form into a more stable twist form at the midpoint of the path. The molecule then proceeds further through a boat transition state, a twist minimum, and a half-chair/sofa transition state before it ends up in the equatorial form.

High-level ab initio calculations were carried out in order to get accurate potential energy differences between the axial and equatorial conformers of all three compounds. Shown in Tables 4−6 are calculated relative energies with thermodynamic

dx.doi.org/10.1021/om4005725 | Organometallics 2013, 32, 6996−7005

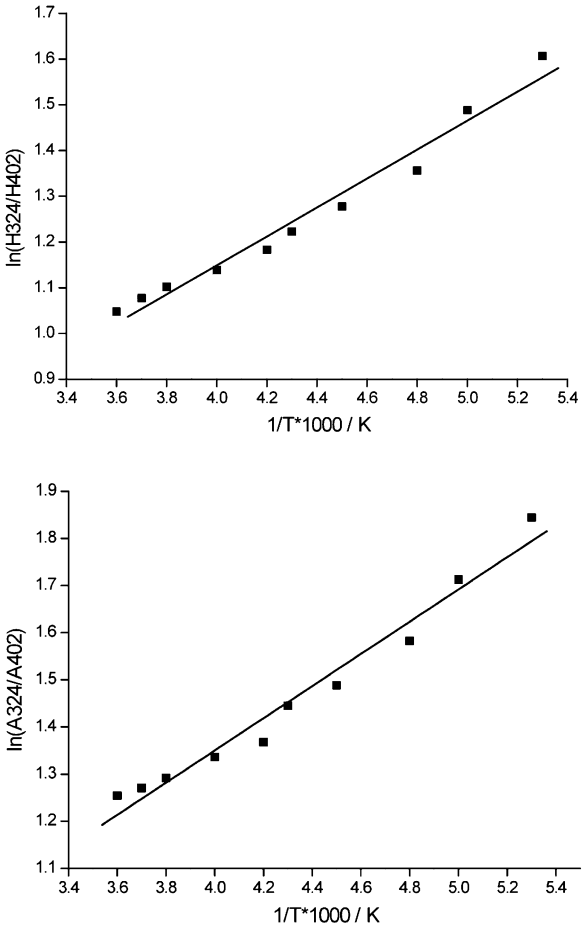

Figure 6. Van't Hoff plots for the 324/402 cm^{-1} band pair of neat $C_5H_{10}SiHI$ using (bottom) band areas and (top) band heights.

corrections at experimental temperatures compared to the experimental (GED, Raman, NMR) energy differences. The 0 K potential energy differences (ZPE-exclusive) evaluated at the CCSD(T)/CBS level of theory for the three compounds as well as the fluoro compound (ΔE = −0.15 kcal/mol) show a trend of increasing stability of the axial conformer in going from the lightest halogen derivative to the heaviest. This trend can also be seen in the values obtained from the various experiments. Overall the agreement with experiment is satisfactory, and we suspect the differences to be mainly due to experimental uncertainties, the imperfect estimations of entropic contributions in the calculations, and solvent effects. The agreement between theory and the Raman experiments is very satisfactory, which may be partly due to the fact that only enthalpic energy differences are being compared (i.e., no entropy effects). There is worse agreement between the theoretical and GED free energy differences for the bromine compound, where a larger population of the axial conformer is found in the GED experiment; however, this is not seen in the low-temperature NMR experiment.

A systematic 0.15−0.19 kcal/mol difference in the low-temperature free energy values from theory and the NMR experiments is evident, although the trend in the values is the same.

We note that we did not attempt to take into account solvent effects in the computations, as such effects are very hard take into account accurately.

A closer look at Tables 4−6 reveals that when the experimental uncertainties are taken into account, all of the experimental and theoretical results for the conformational energy (axial − equatorial) for compounds **8**, **9**, and **10** fit into a remarkably narrow range of −0.50 ± 0.15 kcal mol^{-1}.

In order to better understand the reasons for the conformational preference of 1-halo-1-silacyclohexane molecules we carried out a natural bond order (NBO) analysis.[48−51] With the use of NBO analysis, we performed a decomposition of the total electronic energy into a Lewis component, $E^{(L)}$, and a non-Lewis component, $E^{(NL)}$ (see Table 7). The Lewis component corresponds to the localized structure that has populations of each occupied orbital equal to two electrons. Thus, the Lewis energy nearly exactly incorporates steric and electrostatic interactions and the non-Lewis component corresponds to all types of conjugations.[50,51] It can be seen from the data in Table 7 that on the basis of the non-Lewis components, the effects of conjugations predict the equatorial conformer to be more preferable. Next, NBO analysis was used to calculate the total steric energy.[52−54] It follows from the data shown in Table 7 that the steric energy is considerably higher in the axial conformer than in the equatorial conformer for all compounds. Thus, the axial conformers of 1-X-1-silacyclohexane molecules (X = Cl, Br, I) are examples of stabilization of the form that is unfavorable from the point of view of steric energy and conjugation effects and is determined mainly by electrostatic interactions.

CONCLUSIONS

With this contribution, all 1-halogen-substituted 1-silacyclohexanes have been studied by various experimental techniques and high-level calculations. GED, DNMR, and temperature-dependent Raman experiments all agree that for all of these derivatives the axial conformer is preferred over the equatorial one. This contradicts findings for the corresponding cyclohexane derivatives. For a better comparison of the compounds, we

Table 4. Conformational Properties of $C_5H_{10}SiHCl$ (8)

method	T = 0 K $\Delta E = E_{ax} - E_{eq}$ (kcal mol^{-1})	T = 300−195 K $\Delta H = H_{ax} - H_{eq}$ (kcal mol^{-1})	T = 128.5 K $A = G_{ax} - G_{eq}$ (kcal mol^{-1})	T = 352 K $A = G_{ax} - G_{eq}$ (kcal mol^{-1})
		Calculations		
CCSD(T)/CBS + thermal corr.	−0.54	−0.54	−0.50	−0.43
		Experiments		
GED				−0.43(18)
Raman neat		−0.58(15)		
Raman in heptane		−0.40(15)		
Raman in THF		−0.60(15)		
DNMR			−0.35(6)	

dx.doi.org/10.1021/om4005725 | *Organometallics* 2013, 32, 6996−7005

Table 5. Conformational Properties of $C_5H_{10}SiHBr$ (9)

method	T = 0 K $\Delta E = E_{ax} - E_{eq}$ (kcal mol^{-1})	T = 300−195 K $\Delta H = H_{ax} - H_{eq}$ (kcal mol^{-1})	T = 128.5 K $A = G_{ax} - G_{eq}$ (kcal mol^{-1})	T = 352 K $A = G_{ax} - G_{eq}$ (kcal mol^{-1})
		Calculations		
CCSD(T)/CBS + thermal corr.	−0.62	−0.62	−0.58	−0.49
		Experiments		
GED				−0.82(21)
Raman neat		−0.46(15)		
Raman in heptane		−0.40(15)		
Raman in THF		−0.60(15)		
DNMR			−0.40(3)	

Table 6. Conformational properties of $C_5H_{10}SiHI$ (10)

method	T = 0 K $\Delta E = E_{ax} - E_{eq}$ (kcal mol^{-1})	T = 290−190 K $\Delta H = H_{ax} - H_{eq}$ (kcal mol^{-1})	T = 128.5 K $A = G_{ax} - G_{eq}$ (kcal mol^{-1})	T = 352 K $A = G_{ax} - G_{eq}$ (kcal mol^{-1})
		Calculations		
CCSD(T)/CBS + thermal corr.	−0.63	−0.64	−0.59	−0.48
		Experiments		
GED				−0.59(22)
Raman neat		−0.67(15)		
Raman in toluene		−0.72(15)		
DNMR			−0.40(3)	

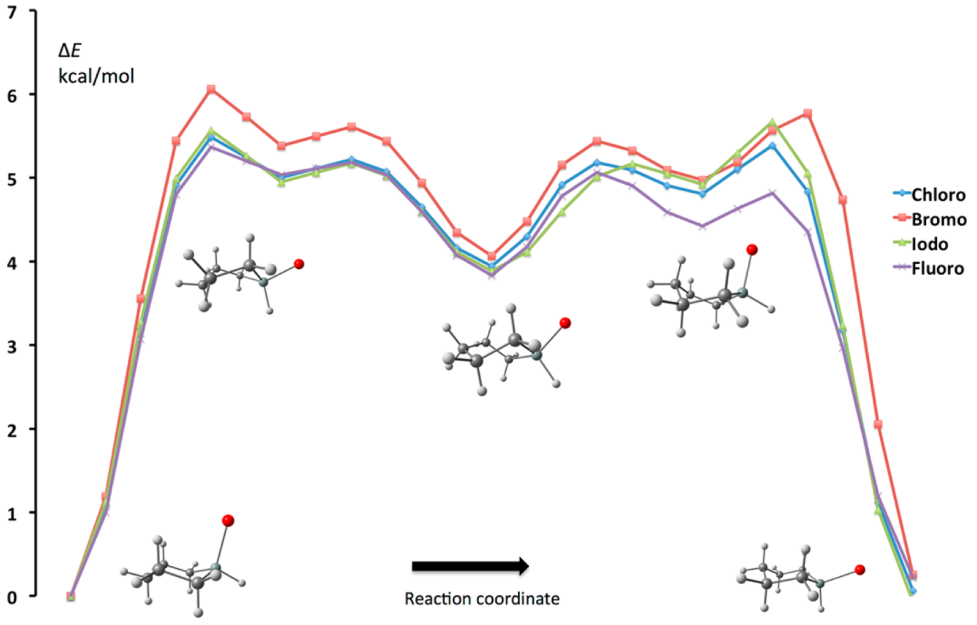

Figure 7. Minimum-energy path for chair-to-chair inversion of compounds **7**−**10**.

have collected the calculated ΔE values at the CCSD(T)/CBS level for both series into one graph (Figure 8). Although the synthesis and conformational experimental analysis on astatine derivatives are not conceivable,[57] we added At derivatives to the calculations to explore further the periodic trend down the halogen group. We may conclude four trends from Figure 8. First, for both series the fluoro derivatives have rather similar energies for the axial and equatorial conformers. Second, for Cl, Br, and I, the cyclohexane derivatives have a distinct preference for the equatorial conformer, whereas the silacyclohexanes have a somewhat stronger preference for the axial conformer. Third, the first two trends are in alignment with the experimental results. Fourth, the calculations predict At to behave in a similar way as Cl, Br, and I.

EXPERIMENTAL SECTION

Materials. The 1-chloro-1-silacyclohexane used as the starting material for the synthesis listed below was prepared in slight variation to the general preparation of silacyclohexanes described by West.[58] It should be pointed out that a mixture of chlorinated and brominated substances is usually obtained by that method because of halogen exchange between the di-Grignard reagent $BrMg(CH_2)_5MgBr$ (or the MgBrCl reaction salt) and $SiHCl_3$ during the reaction. 1-Chloro-1-silacyclohexane and 1-bromo-1-silacyclohexane may be obtained in higher purity by reacting 1-phenyl-1-silacyclohexane with HCl and HBr, respectively. The di-Grignard reagent was prepared in a traditional way. All solvents were dried using appropriate drying agents and distilled prior to use. Standard Schlenk techniques and an inert atmosphere of dry nitrogen were used for all manipulations.

dx.doi.org/10.1021/om4005725 | Organometallics 2013, 32, 6996−7005

Table 7. Results of the NBO Analysis of 1-Halo-1-silacyclohexane Molecules and Energy Decomposition of the Total Electronic Energy $E^{(total)}$ into Lewis $E^{(L)}$, Non-Lewis $E^{(NL)}$, Total Steric $E^{(ST)}$, and Electrostatic $E^{(L-ST)}$ Energies (See the Text)[a]

	Cl		Br		I	
	ax	eq	ax	eq	ax	eq
$\Delta E^{(total)}$	0.0	0.89	0.0	0.83	0.0	0.95
$\Delta E^{(L)}$	0.0	2.73	0.0	2.53	0.0	2.86
$\Delta E^{(NL)}$	1.84	0.0	1.70	0.0	1.91	0.0
$\Delta E^{(ST)}$	3.76	0.0	11.2	0.0	5.41	0.0
$\Delta E^{(L-ST)}$	0.0	6.49	0.0	13.8	0.0	8.27

[a]Relative energies are in kcal mol^{-1}. Calculations were performed at the theoretical levels M06-2X[55]/6-311++G**[40−45] for $C_5H_{10}SiHCl$ and M06-2X/SDB[56]-aug-cc-pVTZ for $C_5H_{10}SiHBr$ and $C_5H_{10}SiHI$.

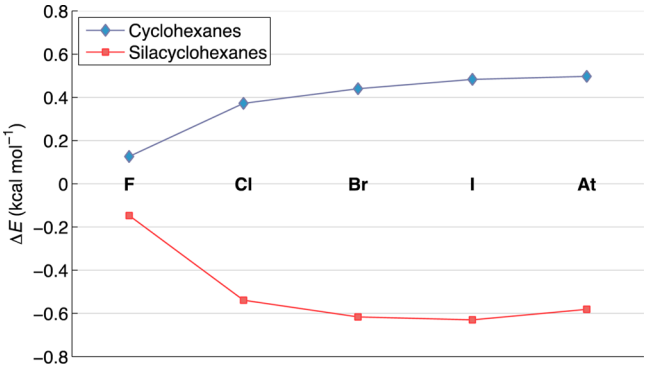

Figure 8. Conformational energies $\Delta E = E_{ax} - E_{eq}$ for $C_6H_{11}X$ and $C_5H_{10}SiHX$.

1-Phenyl-1-silacyclohexane. PhMgBr (14.9 g, 82.0 mmol) was slowly added to 1-chloro-1-silacyclohexane (10.0 g, 74.0 mmol) dissolved in Et_2O (90 mL) while stirring at 0 °C. The diethyl ether was distilled off the reaction mixture and replaced by pentane. The reaction mixture was then filtered under nitrogen and reduced pressure, and the salt was discarded. Distillation of the reaction mixture under reduced pressure (112−115 °C, 25 Torr) yielded 12.4 g (70.0 mmol, 95%) of pure 1-phenyl-1-silacyclohexane.

1-Chloro-1-silacyclohexane (8). Anhydrous HCl (2.4 g, 66.0 mmol) was condensed into a 100 mL ampule containing 1-phenyl-1-silacyclohexane (10.5 g, 60.0 mmol), and the ampule was then sealed off in vacuum. The ampule was inserted in a −78 °C cooling bath (methanol/dry ice bath). Dry ice was added to the cooling bath on a regular basis for the next 2 days. The content of the ampule was then allowed to stand in the cooling bath and slowly warm to room temperature. After the ampule was opened, all of the volatile components were condensed on a N_2(l)-cooled finger. The desired product was collected (after the benzene byproduct had been removed) by distillation under nitrogen at 120−122 °C (4.68 g, 58%) as a colorless liquid. The product was characterized by NMR and MS. ^{1}H NMR (400 MHz, $CDCl_3$): δ 0.94−1.06 (m, 2H, CH_2), 1.32−1.42 (m, 1H, $CH_{2(ax/eq)}$), 1.52−1.60 (m, 1H, $CH_{2(ax/eq)}$), 1.72−1.85 (m, 4H, CH_2), 4.85−4.87 (m, 1H, SiH). ^{13}C{^{1}H} NMR (101 MHz, $CDCl_3$): δ 14.8, 23.1, 29.0. ^{29}Si NMR (79 MHz, $CDCl_3$): δ 7.9. MS (EI, 70 eV) m/z (%): 134 (90), 106 (100), 63 (76). HRMS m/z: calcd for $C_5H_{11}SiCl(35)$ 134.0319, found 134.0312.

1-Bromo-1-silacyclohexane (9). Anhydrous HBr (5.3 g, 66.0 mmol) was condensed into a 100 mL ampule containing 1-phenyl-1-silacyclohexane (10.5 g, 60.0 mmol), and the ampule was then sealed off in vacuum. The ampule was inserted in a −78 °C cooling bath (methanol/dry ice bath). Dry ice was added to the cooling bath on a regular basis for the next 2 days. The content of the ampule was then allowed to stand in the cooling bath and slowly warm to room temperature. After the ampule was opened, all of the volatile components were condensed on a N_2(l)-cooled finger. The desired product was collected (after the benzene byproduct had been removed) by distillation under nitrogen at 138−140 °C (7.78 g, 72%) as a colorless liquid. The product was characterized by NMR and MS. ^{1}H NMR (400 MHz, $CDCl_3$): δ 1.06−1.18 (m, 4H, CH_2), 1.33−1.43 (m, 1H, $CH_{2(ax/eq)}$), 1.54−1.62 (m, 1H, $CH_{2(ax/eq)}$), 1.72−1.87 (m, 4H, CH_2), 4.84−4.86 (m, 1H, SiH). ^{13}C{^{1}H} NMR (101 MHz, $CDCl_3$): δ 14.7, 23.3, 29.0. ^{29}Si NMR (79 MHz, $CDCl_3$): δ −21.9. MS (EI, 70 eV) m/z (%): 178 (79), 150 (100), 109 (54). HRMS m/z: calcd for $C_5H_{11}SiBr(79)$ 177.9813, found 177.9845.

1-Iodo-1-silacyclohexane (10). Iodotrimethylsilane (13.9 g, 69.4 mmol) was slowly added to a solution of 1-chloro-1-silacyclohexane (8.5 g, 63.1 mol) in CH_2Cl_2 (220 mL) under vigorous stirring. After complete addition, the reaction mixture was stirred for 3 days. The desired product was collected (after CH_2Cl_2 had been removed) by distillation under nitrogen at 108−110 °C and 50 Torr (8.10 g, 35.8 mmol, 57%) as a colorless liquid. ^{1}H NMR (400 MHz, $CDCl_3$): δ 1.16−1.24 (m, 2H, $CH_{2(ax/eq)}$), 1.26−1.36 (m, 2H, $CH_{2(ax/eq)}$), 1.37−1.45 (m, 1H, $CH_{2(ax/eq)}$), 1.54−1.64 (m, 1H, $CH_{2(ax/eq)}$), 1.68−1.78 (m, 2H, CH_2), 1.79−1.88 (m, 2H, CH_2), 4.80 (s, $^1J_{H-Si}$ = 224.3 Hz, 1H, SiH). ^{13}C{^{1}H} NMR (101 MHz, $CDCl_3$): δ 14.2, 23.7, 28.9. ^{29}Si{^{1}H} NMR (79 MHz, $CDCl_3$): δ −16.0.

GED Experiments. The electron diffraction patterns of **8** and **9** were recorded at M. V. Lomonosov Moscow State University on the EMR-100 M electron diffraction apparatus. Nozzle temperatures were 46 and 54 °C for **8** and 51 and 54 °C for **9** for the long and short nozzle-to-plate distances, respectively, and an accelerating voltage of about 60 kV and a cubic sector were used. For the scanning on an Epson Perfection 4870 photoscanner, three plates were selected for the long nozzle-to-plate distance (362 mm) and three plates for the short (194 mm) nozzle-to-plate distance. The wavelengths of the electron beam were determined with the use of the scattering pattern from gaseous CCl_4 and were equal to 0.049591 and 0.049402 Å for **8** and 0.049593 and 0.049459 Å for **9** for the long and short nozzle-to-plate distances, respectively. Atomic scattering factors were taken from the International Tables of Crystallography.[59] Experimental backgrounds were drawn as cubic spline functions to the difference between the experimental and theoretical molecular intensity curves with the use of a program developed by A.V.B. Observed intensity curves were recorded in the ranges s = 3.2−19.0 and 7.6−38.0 Å^{-1} for **8** and s = 3.2−19.0 and 7.2−35.0 Å^{-1} for **9** for the long and short nozzle-to-plate distances, respectively. Both curves were digitized with increments of Δs = 0.2 Å^{-1} [$s = (4\pi/\lambda)\sin\theta/2$, where λ is the electron wavelength and θ is the scattering angle]. Least-squares structure refinements were carried out with the use of the computer program KCED25M, which was developed by Norwegian researchers[60,61] and modified by A.V.B. Weight matrices were diagonal. The short-distance data were assigned 0.5 weight and the long-distance data 1.0 weight. Estimated standard deviations calculated by the program were multiplied by a factor of 3 to include added uncertainty due to data correlation and an estimated scale uncertainty of 0.1%.[62] The observed and calculated molecular intensity curves are compared in Figures 9 and 10. The GED experiment for 1-iodo-1-silacyclohexane has been published elsewhere.[31]

Low-Temperature NMR Experiments. A 400 MHz NMR spectrometer (Bruker Avance 400) was used for all of the NMR experiments. A solvent mixture of CD_2Cl_2, $CHFCl_2$, and CHF_2Cl in a ratio of 1:1:3 was used for low-temperature ^{13}C NMR measurements on **8** and **9**. Compound **10** could not be measured in the same freon mixture because of limited solubility at low temperatures. A different solvent mixture of CD_2Cl_2, CHF_2Cl, and CF_3Br in a ratio of 1:2:2 allowed us to perform measurements on **10** successfully. The temperature of the probe was calibrated by means of a type K (chromel/alumel) thermocouple inserted into a dummy tube. The readings are estimated to be accurate within ±2 K. The NMR spectra were loaded into the data-handling program IGOR (WaveMetrics) for analysis, manipulations, and graphic display. Line shape simulations of the NMR spectra were performed using the WinDNMR program.[36]

dx.doi.org/10.1021/om4005725 | Organometallics 2013, 32, 6996−7005

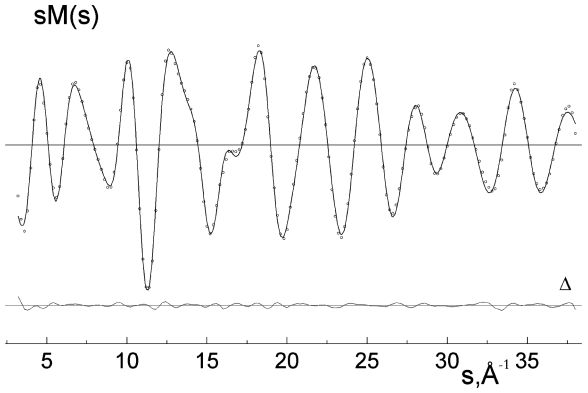

Figure 9. (top) Experimental (open circles) and calculated (solid line) molecular intensity curves for $C_5H_{10}SiHCl$. (bottom) Difference curve for the optimized mixture of the conformers.

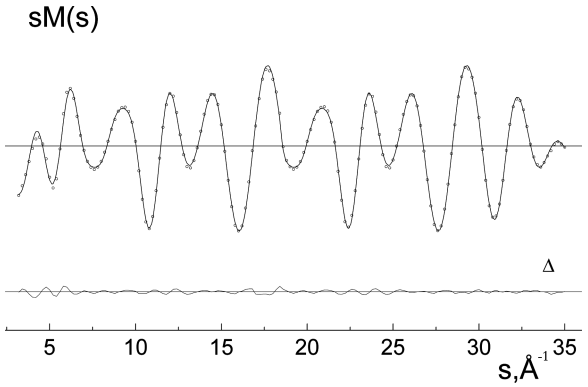

Figure 10. (top) Experimental (open circles) and calculated (solid line) molecular intensity curves for $C_5H_{10}SiHBr$. (bottom) Difference curve for the optimized mixture of the conformers.

Low-Temperature Raman Experiments. Raman spectra were recorded with a Jobin Yvon T64000 spectrometer equipped with a triple monochromator and a CCD camera. The samples were filled into 1 mm capillary glass tubes and irradiated by the green 532 nm line of a frequency-doubled Nd:YAG laser (Coherent, DPSS model 532-20, 10 mW). Spectra were recorded from pure compound and in heptane and THF solutions. A continuous-flow cryostat (Oxford Instruments OptistatCF) using liquid nitrogen for cooling was employed for the low-temperature measurements.

COMPUTATIONAL DETAILS

All of the calculations for direct comparison and use with GED experiments were carried out at the MP2(full)/SDB-aug-cc-pVTZ level of theory for Br and I atoms and the MP2(full)/aug-cc-PVTZ level of theory for all other atoms. The theoretical molecular force fields were used to calculate mean vibrational amplitudes and vibrational correction terms necessary for GED analysis. To reduce the number of refined parameters, the following assumptions were made on the basis of MP2 results. Only the geometric parameters of the axial conformer were refined, and the parameters of the equatorial form were tied to those of the axial conformer using the calculated differences. For the axial conformer, the difference between the nearly equal C2−C3 and C3−C4 bond lengths was constrained to the calculated value. All of the C−H bonds, the H−C−H angles, and the H_{ax}−C2−C3, H_{eq}−C3−C2, H_{eq}−C3−C4, and H_{ax}−C3−C2 angles were set equal. Angles that define the orientation of the C−H bonds were set to calculated values. The optimized theoretical geometry parameters were found to be in good agreement with experimental ones.

The minimum-energy pathways for the chair-to-chair inversions of compounds **7**−**10** were calculated in redundant internal coordinates with the STQN(Path)[63] method as implemented in Gaussian 09[64] at the B3LYP/6-31G(d)[40−45] level of theory (def2-SVP basis set and ECP used for iodine[65]).

High-level ab initio calculations were carried out on MP2/cc-pVTZ[46,47] optimized geometries (using the cc-pVTZ-PP and ECP on I and At[66]). The energy differences at the CCSD(T)/CBS (CBS = complete basis set) level were then estimated by performing large-basis MP2 calculations that were extrapolated to the basis set limit and then applying a CCSD(T) correction to the MP2/CBS value:

$$\Delta E^{\mathrm{CCSD(T)/CBS}} \approx \Delta E^{\mathrm{MP2/CBS}} + (\Delta E^{\mathrm{CCSD(T)/small\ basis}} - \Delta E^{\mathrm{MP2/small\ basis}})$$

The MP2 calculations were performed with correlation-consistent basis sets up to the aug-cc-pV5Z level (using the aug-cc-pVXZ-PP basis set and ECP for iodine and astatine). The energy difference obtained at the MP2/aug-cc-pV5Z level was estimated as being sufficiently close to the basis set limit, MP2/CBS. The $(\Delta E^{\mathrm{CCSD(T)/small\ basis}} - \Delta E^{\mathrm{MP2/small\ basis}})$ term was calculated at the CCSD(T)/aug-cc-pVTZ and MP2/aug-cc-pVTZ levels. All of the MP2 and CCSD(T) calculations performed with Molpro 2006.1.[67] Thermal corrections to enthalpies and free energies were calculated from B97-1[68]/def2-TZVPP[65] harmonic vibrational frequencies (accompanying def2 ECP on iodine). This CCSD(T)/CBS protocol has been used in previous studies on silacyclohexanes.[17]

All of the enthalpy and entropy corrections to the conformational energies were calculated at the same level (B97-1/def2-TZVPP) for consistency. The B97-1 functional is known to predict good harmonic frequencies and enthalpy and entropy corrections.[69] A problem with harmonic frequency calculations for six-membered rings persists, however. Six-membered rings include a number of low-frequency vibrations that are known to be badly predicted by the harmonic approximation. As they contribute significantly to the entropy, errors in the entropy correction and hence the computed free energy differences can be expected. The absolute ^{13}C NMR shielding constants of the carbon nuclei were calculated with the GIAO method[70,71] using the PBE1 functional[72−74] and a mixed basis set consisting of aug-pcS-2[75] on carbon atoms and def2-TZVPP on all other atoms (including the def2 ECP on iodine). Shielding constants were converted to chemical shifts by reference to ^{13}C shielding constants in TMS. All of the geometries (including the TMS standard) were optimized at the MP2/cc-pVTZ level. The magnitudes of the relative shieldings are in reasonable agreement with experiment (slight overestimation), and their signs confirmed the expected assignment in which the ring carbon nuclei (apart from C4) are more shielded in the axial conformer than in the equatorial one. All of the calculated ^{13}C NMR shielding constants are available in the Supporting Information.

ASSOCIATED CONTENT

Supporting Information

Simulated spectra and parameters derived from the DNMR analysis, NMR spectra (^1H and ^{13}C) for the title compounds, selected Raman spectra, figures showing deconvolution of signals and van't Hoff plots, calculated ^{13}C NMR chemical shifts for the title compounds, MP2-optimized geometries, and a file of all computed Cartesian coordinates in a format for convenient visualization. This material is available free of charge via the Internet at http://pubs.acs.org.

AUTHOR INFORMATION

Corresponding Author

*E-mail: ingvara@hi.is.

Present Addresses

[⊥]ICI Rheocenter, Reykjavik University, Innovation Center Iceland, Keldnaholti, IS-112 Reykjavik, Iceland.

[#]Max-Planck Institute for Chemical Energy Conversion, Stiftstrasse 32-34, D-45470 Mülheim an der Ruhr, Germany.
[▽]Takeda Austria GmbH, St. Peter-Straße 25, A-4020 Linz, Austria.

Notes

The authors declare no competing financial interest.
[†]Conformations of Silicon-Containing Rings. 11. For Part 10, see ref 1.

■ ACKNOWLEDGMENTS

Financial support from RANNÍS – The Icelandic Centre for Research (Grant 080038021) is gratefully acknowledged. Use of the computing resources of the EaStCHEM Research Computing Facility are acknowledged. A.V.B. is grateful to RFBR (Project 12-03-91330-NNIOa) and the Government of RF (Project 11.G34.31.0069) for financial support. T.K. and K.H. thank the Austrian Science Foundation FWF (Fonds zur Förderung der wissenschaftlichen Forschung, Vienna) for financial support of Project P 21272-N19.

■ REFERENCES

(1) Arnason, I.; Gudnason, P. I.; Björnsson, R.; Oberhammer, H. *J. Phys. Chem. A* **2011**, *115*, 10000.
(2) Eliel, E. L.; Wilen, S. H. *Stereochemistry of Organic Compounds*; Wiley: New York, 1994.
(3) *Conformational Behavior of Six-Membered Rings: Analysis, Dynamics, and Stereoelectronic Effects*; Juaristi, E., Ed.; Methods in Stereochemical Analysis; VCH: New York, 1995.
(4) Arnason, I.; Kvaran, Á.; Bodi, A. *Int. J. Quantum Chem.* **2006**, *106*, 1975.
(5) Arnason, I.; Thorarinsson, G. K.; Matern, E. *Z. Anorg. Allg. Chem.* **2000**, *626*, 853.
(6) Winstein, S.; Holness, N. J. *J. Am. Chem. Soc.* **1955**, *77*, 5562.
(7) Burkert, U.; Allinger, N. L. *Molecular Mechanics*; ACS Monograph *177*; American Chemical Society: Washington, DC, 1982.
(8) Booth, H.; Everett, J. R. *J. Chem. Soc., Perkin Trans. 2* **1980**, 255.
(9) Bushweller, C. H. Stereodynamics of Cyclohexane and Substituted Cyclohexanes. Substituent *A* Values. In *Conformational Behavior of Six-Membered Rings: Analysis, Dynamics, and Stereoelectronic Effects*; Juaristi, E., Ed.; Methods in Stereochemical Analysis; VCH: New York, 1995; pp 25.
(10) Manharan, M.; Eliel, E. L. *Tetrahedron Lett.* **1984**, *25*, 3267.
(11) Wiberg, K. B.; Hammer, J. D.; Castejon, H.; Bailey, W. F.; DeLeon, E. L.; Jarret, R. M. *J. Org. Chem.* **1999**, *64*, 2085.
(12) Taddei, F.; Kleinpeter, E. *J. Mol. Struct.: THEOCHEM* **2004**, *683*, 29.
(13) Taddei, F.; Kleinpeter, E. *J. Mol. Struct.: THEOCHEM* **2005**, *718*, 141.
(14) Cortés-Guzmán, F.; Hernández-Trujillo, J.; Cuevas, G. *J. Phys. Chem. A* **2003**, *107*, 9253.
(15) Arnason, I.; Kvaran, A.; Jonsdottir, S.; Gudnason, P. I.; Oberhammer, H. *J. Org. Chem.* **2002**, *67*, 3827.
(16) Favero, L. B.; Velino, B.; Caminati, W.; Arnason, I.; Kvaran, A. *Organometallics* **2006**, *25*, 3813.
(17) Kern, T.; Hölbling, M.; Dzambaski, A.; Flock, M.; Hassler, K.; Wallevik, S. Ó.; Arnason, I.; Bjornsson, R. *J. Raman Spectrosc.* **2012**, *43*, 1337.
(18) Klaeboe, P.; Horn, A.; Nielsen, C. J.; Aleksa, V.; Guirgis, G. A.; Wyatt, J. K.; Dukes, H. W. *J. Mol. Struct.* **2013**, *1034*, 207.
(19) Shainyan, B. A.; Kleinpeter, E. *Tetrahedron* **2012**, *68*, 114.
(20) Durig, J. R.; El Defrawy, A. M.; Ward, R. M.; Guirgis, G. A.; Gounev, T. K. *Struct. Chem.* **2008**, *19*, 579.
(21) Eliel, E. L.; Manoharan, M. *J. Org. Chem.* **1981**, *46*, 1959.
(22) Squillacote, M. E.; Neth, J. M. *J. Am. Chem. Soc.* **1987**, *109*, 198.
(23) Girichev, G. V.; Giricheva, N. I.; Bodi, A.; Gudnason, P. I.; Jonsdottir, S.; Kvaran, A.; Arnason, I.; Oberhammer, H. *Chem.—Eur. J.* **2007**, *13*, 1776.
(24) Girichev, G. V.; Giricheva, N. I.; Bodi, A.; Gudnason, P. I.; Jonsdottir, S.; Kvaran, A.; Arnason, I.; Oberhammer, H. *Chem.—Eur. J.* **2009**, *15*, 8929.
(25) Wallevik, S. Ó.; Bjornsson, R.; Kvaran, Á.; Jonsdottir, S.; Arnason, I.; Belyakov, A. V.; Baskakov, A. A.; Hassler, K.; Oberhammer, H. *J. Phys. Chem. A* **2010**, *114*, 2127.
(26) Bjornsson, R.; Arnason, I. *Phys. Chem. Chem. Phys.* **2009**, *11*, 8689.
(27) Bodi, A.; Bjornsson, R.; Arnason, I. *J. Mol. Struct.* **2010**, *978*, 14.
(28) Bodi, A.; Kvaran, Á.; Jonsdottir, S.; Antonsson, E.; Wallevik, S. Ó.; Arnason, I.; Belyakov, A. V.; Baskakov, A. A.; Hölbling, M.; Oberhammer, H. *Organometallics* **2007**, *26*, 6544.
(29) Favero, L. B.; Velino, B.; Caminati, W.; Arnason, I.; Kvaran, A. *J. Phys. Chem. A* **2006**, *110*, 9995.
(30) Klaeboe, P.; Aleska, V.; Nielsen, C. J.; Horn, A.; Guirgis, G. A.; Johnston, M. D. *J. Mol. Struct.* **2012**, *1015*, 120.
(31) Belyakov, A. V.; Baskakov, A. A.; Berger, R. J. F.; Mitzel, N. W.; Oberhammer, H.; Arnason, I.; Wallevik, S. Ó. *J. Mol. Struct.* **2012**, *1012*, 126.
(32) Belyakov, A. V.; Baskakov, A. A.; Naraev, V. N.; Rykov, A. N.; Oberhammer, H.; Arnason, I.; Wallevik, S. O. *Russ. J. Gen. Chem.* **2011**, *81*, 2257.
(33) Belyakov, A. V.; Baskakov, A. A.; Naraev, V. N.; Rykov, A. N.; Oberhammer, H.; Arnason, I.; Wallevik, S. O. *Russ. J. Phys. Chem. A* **2012**, *86*, 1563.
(34) Aleksa, V.; Guirgis, G. A.; Horn, A.; Klaeboe, P.; Liberatore, R. J.; Nielsen, C. J. *Vib. Spectrosc.* **2012**, *61*, 167.
(35) Bent, H. A. *Chem. Rev.* **1961**, *61*, 275.
(36) Reich, H. J. WinDNMR: Dynamic NMR Spectra for Windows; *J. Chem. Educ. Software 3D2*.
(37) Wallevik, S. Ó.; Bjornsson, R.; Kvaran, Á.; Jonsdottir, S.; Girichev, G. V.; Giricheva, N. I.; Hassler, K.; Arnason, I. *J. Mol. Struct.* **2010**, *978*, 209.
(38) Becke, A. D. *J. Chem. Phys.* **1993**, *98*, 5648.
(39) Lee, C.; Yang, W.; Parr, R. G. *Phys. Rev. B* **1988**, *37*, 785.
(40) Binning, R. C., Jr.; Curtiss, L. A. *J. Comput. Chem.* **1990**, *11*, 1206.
(41) Clark, T.; Chandrasekhar, J.; Spitznagel, G. W.; Schleyer, P. v. R. *J. Comput. Chem.* **1983**, *4*, 294.
(42) Hariharan, P. C.; Pople, J. A. *Theor. Chim. Acta* **1973**, *28*, 213.
(43) Hehre, W. J.; Ditchfield, R.; Pople, J. A. *J. Chem. Phys.* **1972**, *56*, 2257.
(44) McLean, A. D.; Chandler, G. S. *J. Chem. Phys.* **1980**, *72*, 5639.
(45) Raghavachari, K.; Binkley, J. S.; Seeger, R.; Pople, J. A. *J. Chem. Phys.* **1980**, *72*, 650.
(46) Dunning, T. H., Jr. *J. Chem. Phys.* **1989**, *90*, 1007.
(47) Woon, D. E.; Dunning, T. H., Jr. *J. Chem. Phys.* **1993**, *98*, 1358.
(48) Foster, J. P.; Weinhold, F. *J. Am. Chem. Soc.* **1980**, *102*, 7211.
(49) Glendening, E. D.; Landis, C. R.; Weinhold, F. *Wiley Interdiscip. Rev.: Comput. Mol. Sci.* **2012**, *2*, 1.
(50) Weinhold, F. *Discovering Chemistry With Natural Bond Orbitals*; Wiley: Hoboken, NJ, 2012.
(51) Weinhold, F.; Landis, C. R. *Valency and Bonding: A Natural Bond Orbital Donor-Acceptor Perspective*; Cambridge University Press: Cambridge, U.K., 2005.
(52) Badenhoop, J. K.; Weinhold, F. *J. Chem. Phys.* **1997**, *107*, 5406.
(53) Badenhoop, J. K.; Weinhold, F. *J. Chem. Phys.* **1997**, *107*, 5422.
(54) Badenhoop, J. K.; Weinhold, F. *Int. J. Quantum Chem.* **1999**, *72*, 269.
(55) Zhao, Y.; Truhlar, D. G. *Theor. Chem. Acc.* **2008**, *120*, 215.
(56) Martin, J. M. L.; Sundermann, A. *J. Chem. Phys.* **2001**, *114*, 3408.
(57) Greenwood, N. N.; Earnshaw, A. *Chemistry of the Elements*, 2nd ed.; Elsevier Butterworth-Heinemann: Oxford, U.K., 1997.
(58) West, R. *J. Am. Chem. Soc.* **1954**, *76*, 6012.
(59) Ross, A. W.; Fink, M.; Hilderbrandt, R. L. *International Tables of Crystallography, C*; Kluwer: Dordrecht, The Netherlands, 1992.

(60) Andersen, B.; Seip, H. M.; Strand, T. G.; Stolevik, R. *Acta Chem. Scand.* **1969**, *23*, 3224.
(61) Gundersen, G.; Samdal, S.; Seip, H. M. *Least Squares Structural Refinement Program Based on Gas Electron-Diffraction Data*; Department of Chemistry, University of Oslo: Oslo, Norway, 1981; Vols. *I*–*III*.
(62) Golubinskii, A. V.; Vilkov, L. V.; Mastryukov, V. S.; Novikov, V. P. *Vestn. Mosk. Univ., Ser. 2: Khim.* **1979**, *20*, 99.
(63) Ayala, P. Y.; Schlegel, H. B. *J. Chem. Phys.* **1997**, *107*, 375.
(64) Frisch, M. J.; Trucks, G. W.; Schlegel, H. B.; Scuseria, G. E.; Robb, M. A.; Cheeseman, J. R.; Scalmani, G.; Barone, V.; Mennucci, B.; Petersson, G. A.; Nakatsuji, H.; Caricato, M.; Li, X.; Hratchian, H. P.; Izmaylov, A. F.; Bloino, J.; Zheng, G.; Sonnenberg, J. L.; Hada, M.; Ehara, M.; Toyota, K.; Fukuda, R.; Hasegawa, J.; Ishida, M.; Nakajima, T.; Honda, Y.; Kitao, O.; Nakai, H.; Vreven, T.; Montgomery, J. A., Jr.; Peralta, J. E.; Ogliaro, F.; Bearpark, M.; Heyd, J. J.; Brothers, E.; Kudin, K. N.; Staroverov, V. N.; Kobayashi, R.; Normand, J.; Raghavachari, K.; Rendell, A.; Burant, J. C.; Iyengar, S. S.; Tomasi, J.; Cossi, M.; Rega, N.; Millam, N. J.; Klene, M.; Knox, J. E.; Cross, J. B.; Bakken, V.; Adamo, C.; Jaramillo, J.; Gomperts, R. E.; Stratmann, O.; Yazyev, A. J.; Austin, R.; Cammi, C.; Pomelli, J. W.; Ochterski, R.; Martin, R. L.; Morokuma, K.; Zakrzewski, V. G.; Voth, G. A.; Salvador, P.; Dannenberg, J. J.; Dapprich, S.; Daniels, A. D.; Farkas, Ö.; Foresman, J. B.; Ortiz, J. V.; Cioslowski, J.; Fox, D. J. Gaussian 09, revision A.02; Gaussian, Inc.: Wallingford, CT, 2009.
(65) Weigend, F.; Ahlrichs, R. *Phys. Chem. Chem. Phys.* **2005**, *7*, 3297.
(66) Peterson, K. A.; Shepler, B. C.; Figgen, D.; Stoll, H. *J. Phys. Chem. A* **2006**, *110*, 13877.
(67) Werner, H.-J.; Knowles, P. J.; Knizia, G.; Manby, F. R.; Schütz, M. *Wiley Interdiscip. Rev.: Comput. Mol. Sci.* **2012**, *2*, 242.
(68) Hamprecht, F. A.; Cohen, A.; Tozer, D. J.; Handy, N. C. *J. Chem. Phys.* **1998**, *109*, 6264.
(69) Merrick, J. P.; Moran, D.; Radom, L. *J. Phys. Chem. A* **2007**, *111*, 11683.
(70) Dichtfield, R. *Mol. Phys.* **1974**, *27*, 789.
(71) Wolinski, K.; Hinton, J. F.; Pulay, P. J. *J. Am. Chem. Soc.* **1990**, *112*, 8251.
(72) Adamo, C.; Barone, V. *J. Chem. Phys.* **1999**, *110*, 6158.
(73) Perdew, J. P.; Burke, K.; Ernzerhof, M. *Phys. Rev. Lett.* **1996**, *77*, 3865.
(74) Perdew, J. P.; Burke, K.; Ernzerhof, M. *Phys. Rev. Lett.* **1997**, *78*, 1396.
(75) Jensen, F. *J. Chem. Theory. Comput.* **2008**, *4*, 719.